Assessment and Evaluation of Single Phase Grid Linked Transformer less Inverter with PV Input

Y.Vishnu Vardhan
M.Tech (Power Electronics)
Department of EEE,
Prasad Engineering College.

S.Sahithi
Associate Professor & HoD,
Department of EEE,
Prasad Engineering College.

Abstract:

Single-phase transformer less inverter is widely used in low-power photovoltaic (PV) grid-connected systems due to its small size, high efficiency and low cost. When no transformer is used in a grid connected photovoltaic (PV) system, a galvanic connection between the grid and PV array exists. In these conditions, dangerous leakage currents (common-mode currents) can appear through the stray capacitance between the PV array and the ground. The former, in order to create a galvanic isolation between the input and the output include a transformer (mandatory in some countries) that limits the whole system performances in terms of efficiency, weight, size and cost. On the contrary, transformer-less inverters do not present any isolation and are characterized by little size, lower cost and higher efficiency (more than 2% higher). Nevertheless, the lack of transformers leads to leakage currents that can be harmful to the human body, as well as for the whole conversion system integrity. In this paper it presents a high-reliability single-phase transformer less grid-connected inverter that operate super junction MOSFETs to accomplish high efficiency for photovoltaic applications.

Index Terms- photovoltaic (PV) grid-connected system, Single-phase transformerless inverter, PWM control

INTRODUCTION

In recent past years the photovoltaic (PV) systems have been received unprecedented concentration due to the raise of concerns about adverse effects of extensive use of fossil fuels on the environment and energy utilization with security in grid-connected PV systems that are still outnumbered by the power generation schemes which are based on oil or natural gas or coal or nuclear or hydro or wind or any combination of these [1] PV systems capacity is majorly based on the order of tens of megawatts that have been installed and interfaced at the grid level in the primary distribution where the PV system installation at the secondary distribution level are dominated by rooftop units with distinct capacities on the order of a few kilowatts with no significant impact on the existing power systems. An attractive feature of PV systems is that they produce electric power without harming the environment, by directly transforming a free unlimited source of energy, solar radiation, into electricity. This fact along with the continuing decrease in PV arrays cost and the increase in their efficiency has resulted in the use of PV generation systems. In the past, PV sources were commonly used in isolated and stand-alone applications. Nowadays, the trend is to connect the PV systems to the public grid, selling the generated power with advantageous price ratings fixed by governmental policies.

High frequency common-mode (CM) voltages must be avoided for a transformerless PV grid-connected inverter because it will lead to a large charge/discharge current partially flowing through the inverter to the ground. This CM ground current will cause an increase in the current harmonics, higher losses, safety problems, and electromagnetic interference (EMI) issues For a grid-connected PV system, energy yield and payback time are greatly dependant on the inverter's reliability and efficiency, which are regarded as two of the most significant characteristics for PV

inverters. In order to minimize the ground leakage current and improve the efficiency of the converter system, transformerless PV inverters utilizing unipolar PWM control have been presented [8]–[10]. The weighted California Energy Commission (CEC) or European Union (EU) efficiencies of most commercially available and literature-reported single-phase PV transformerless inverters are in the range of 96–98%.

The reported system peak and CEC efficiencies with an 8-kW converter system from the product datasheet is 98.3% and 98%, respectively, with 345-V dc input voltage and a 16-kHz switching frequency. However, this topology has high conduction losses due to the fact that the current must conduct through three switches in series during the active phase. Another disadvantage of the H5 is that the line-frequency switches S1 and S2 cannot utilize MOSFET devices because of the MOSFET body diode's slow reverse recovery. Replacing the switch S5 of the H5 inverter with two split switches S5 and S6 into two phase legs and adding two freewheeling diodes D5 and D6 for freewheeling current flows, the H6 topology was proposed in [12]. The H6 inverter can be implemented using MOSFETs for the line frequency switching devices, eliminating the use of less efficient IGBTs. The reported peak efficiency and EU efficiency of a 300 W prototype circuit were 98.3% and 98.1%, respectively, with 180 V dc input voltage and 30 kHz switching frequency. The fixed voltage conduction losses of the IGBTs used in the H5 inverter are avoided in the H6 inverter topology improving efficiency; however, there are higher conduction losses due to the three series-connected switches in the current path during active phases. The shoot-through issues due to three active switches series connected to the dc-bus still remain in the H6 topology. Another disadvantage to the H6 inverter is that when the inverter output voltage and current has a phase shift the MOSFET body diodes may be activated. This can cause body diode reverse-recovery issues and decrease the reliability of the system.
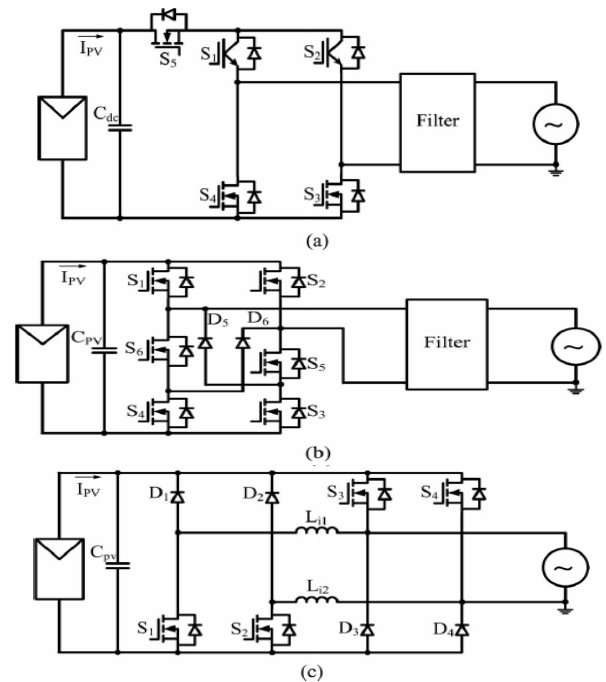
Fig. 1 Single-phase transformerless PV inverters using super junction MOSFETs: (a) H5, (b) H6, and (c) dual-paralleled-buck inverters

Another high-efficiency transformerless MOSFET inverter topology is the dual-paralleled-buck converter, as shown in Fig. 1(c). The dual-parallel-buck converter was inversely derived from the dual-boost bridgeless power-factor correction (PFC) circuit in [13]. The dual-paralleled-buck inverter eliminates the problem of high conduction losses in the H5 and H6 inverter topologies because there are only two active switches in series with the current path during active phases. The reported maximum and EU efficiencies of the dual-paralleled-buck inverter using Cool MOS switches and SiC diodes tested on a 4.5 kW prototype circuit were 99% and 98.8%, respectively, with an input voltage of 375 V and a switching frequency at 16 kHz. The main issue of this topology is that the grid is directly connected by two active switches S3 and S4 , which may cause a grid short-circuit problem, reducing the reliability of the topology. A dead time of 500 μs between the line-frequency switches S3 and S4 at the zero-crossing instants needed to be added to avoid grid shoot-through.

This adjustment to improve the system reliability comes at the cost of high zero-crossing distortion for the output grid current. One key issue for a high efficiency and reliability transformerless PV inverter is that in order to achieve high efficiency over a wide load range it is necessary to utilize MOSFETs for all switching devices. Another key issue is that the inverter should not have any shoot-through issues for higher reliability. In order to address these two key issues, a new inverter topology is proposed for single-phase transformerless PV grid-connected systems in this paper. The proposed transformerless PV inverter features: 1) high reliability because there are no shoot-through issues, 2) low output ac current distortion as a result of no dead-time requirements at every PWM switching commutation instant as well as at grid zero-crossing instants, 3) minimized CM leakage current because there are two additional ac-side switches that decouple the PV array from the grid during the freewheeling phases, and 4) all the active switches of the proposed converter can reliably employ super junction MOSFETs since it never has the chance to induce MOSFET body diode reverse recovery. As a result of the low conduction and switching losses of the superjunction MOSFETs, the proposed converter can be designed to operate at higher switching frequencies while maintaining high system efficiency. Higher switching frequencies reduce the ac-current ripple and the size of passive components.

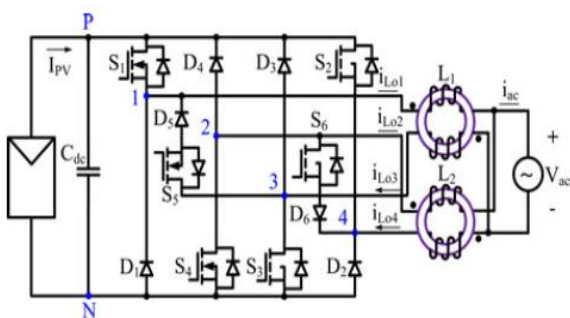## PROPOSED TOPOLOGY AND OPERATION ANALYSIS

Fig.2 proposed high efficiency and reliability PV transform less inverter topology

Fig. 2 shows the circuit diagram of the proposed transformerless PV inverter, which is composed of six MOSFETs switches (S1–S6), six diodes (D1–D6), and two split ac-coupled inductors L1 and L2 . The diodesD1–D4 perform voltage clamping functions for active switches S1–S4 . The ac-side switch pairs are composed of S5, D5 and S6, D6, respectively, which provide unidirectional current flow branches during the freewheeling phases decoupling the grid from the PV array and minimizing the CM leakage current. Compared to the HERIC topology [9] the proposed inverter topology divides the ac side into two independent units for positive and negative half cycle. In addition to the high efficiency and low leakage current features, the proposed transformerless inverter avoids shoot-through enhancing the reliability of the inverter. The inherent structure of the proposed inverter does not lead itself to the reverse recovery issues for the main power switches and as such superjunction MOSFETs can be utilized without any reliability or efficiency penalties.
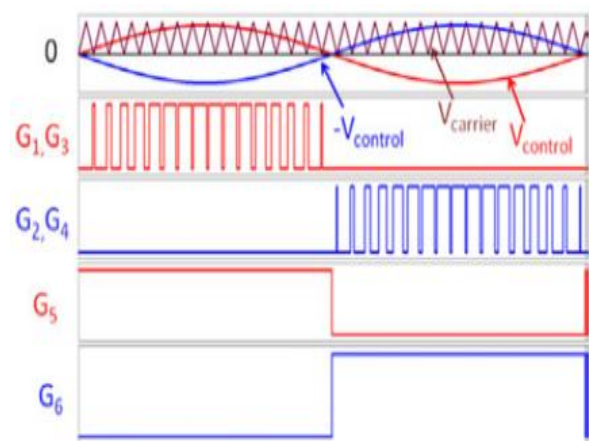

Fig. 3 illustrates the PWM scheme for the proposed inverter.

When the reference signal Vcontrol is higher than zero, MOSFETs S1 and S3 are switched simultaneously in the PWMmode and S5 is kept on as a polarity selection switch in the half grid cycle; the gating signals G2, G4 , and G6 are low and S2, S4 , and S6 are inactive. Similarly, if the reference signal –Vcontrol is higher than zero, MOSFETs S2 and S4 are switched simultaneously in the PWM mode and S6 is

on as a polarity selection switch in the grid cycle; the gating signals G1, G3 , and G5 are low and S1, S3, and S5 are inactive.
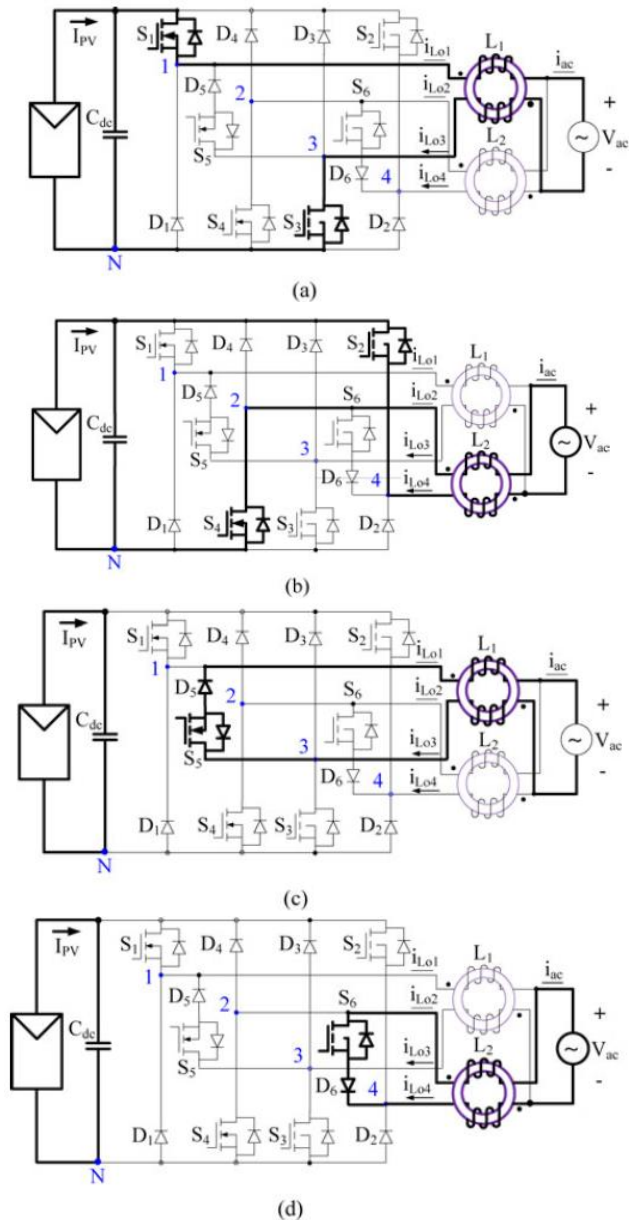

Fig.4 Topological stages of the proposed inverter: (a) active stage of positive half-line cycle, (b) freewheeling stage of positive half-line cycle, (c) active stage of negative half-line cycle, and (d) freewheeling stage of negative half-line cycle

Fig. 4 shows the four operation stages of the proposed inverter within one grid cycle. In the positive half-line grid cycle, the high-frequency switches S1 and S3 are modulated by the sinusoidal reference signal Vcontrol while S5 remains turned ON. When S1 and S3 are ON, diode D5 is reverse-biased, the inductor currents of iLo1 and iLo3 are equally charged, and energy is transferred from the dc source to the grid; when S1 and S3 are deactivated, the switch S5 and diode D5 provide the inductor current iL1 and iL3 a freewheeling path decoupling the PV panel from the grid to avoid the CM leakage current. Coupled-inductor L2 is inactive in the positive half-line grid cycle. Similarly, in the negative half cycle, S2 and S4 are switched at high frequency and S6 remains ON. Freewheeling occurs through S6 and D6.

Ground Loop Leakage Current Analysis for the Proposed Transformerless Inverter

A galvanic connection between the ground of the grid and the PV array exists in transformerless grid-connected PV systems. Large ground leakage currents may appear due to the high stray capacitance between the PV array and the ground. In order to analyze the ground loop leakage current, Fig. 5 shows a model with the phase output points 1, 2, 3, and 4 modeled as controlled voltage sources connected to the negative terminal of the dc bus (N point). Fig. 5 clearly illustrates the stray elements influencing the ground leakage current, which include: 1) the stray capacitance between PV array and ground CPVg ; 2) stray capacitances between the inverter devices and the ground Cg1 − Cg4 ; and 3) the series impedance between the ground connection points of the inverter and the grid Zg. The differential-mode (DM) filter capacitor Cx and the CM filter components LCM, CY 1 , and CY 2 are also shown in the model. The value of the stray capacitances Cg1, Cg2, Cg3 , and Cg4 of MOSFETs is very low compared with that of CPVg , therefore the influence of these capacitors on the leakage current can be neglected. It is also noticed that the DM capacitor Cx does not affect the CM leakage current. Moreover, during the positive half-line cycle, switches S2, S4 , and S6 are kept deactivated; hence the controlled voltage sources V2N and V4N are equal to zero and can be removed. Consequently, a

simplified CM leakage current model for the positive half-line cycle is derived as shown in Fig. 6.
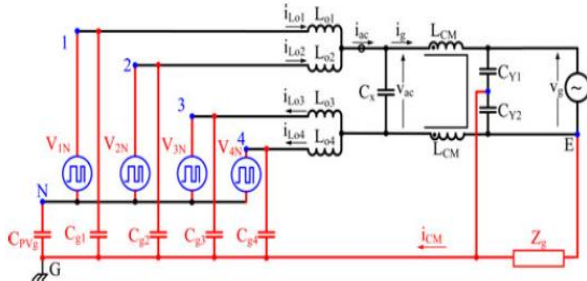

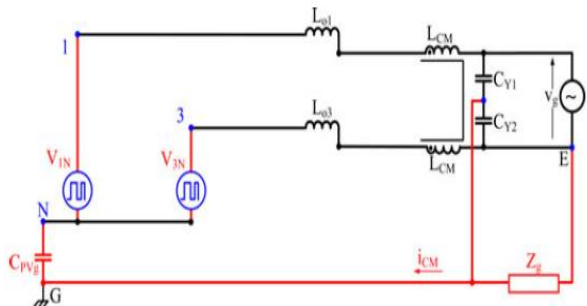Fig.5 Leakage current analysis model for the proposed transformerless PV inverter

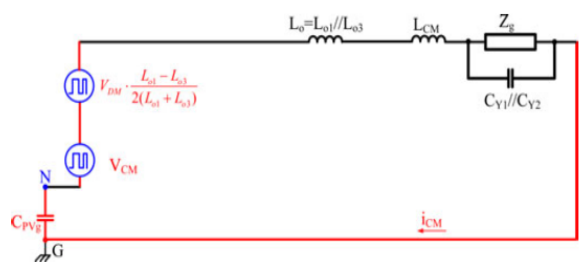Fig. 6 Simplified CM leakage current analysis model for positive half-line cycle

Fig.7 Simplified single-loop CM model for positive half-line cycle

With the help of the CM and DM concepts and by introducing the equivalent circuits between N and E, a single-loop mode applicable to the CM leakage current analysis for the positive half-line cycle of the proposed transformerless inverter is obtained, as shown in Fig. 7, with

$$V_{CM} = \frac{V_{1N} + V_{3N}}{2} \quad (1)$$

$$V_{DM} = V_{1N} - V_{3N} \quad (2)$$

A total CM voltage V_{tCM} is defined as

$$V_{tCM} = V_{CM} + V_{DM} \cdot \frac{L_{o1} - L_{o3}}{2(L_{o1} + L_{o3})} = \frac{V_{1N} + V_{3N}}{2}$$
$$+ (V_{1N} - V_{3N}) \cdot \frac{L_{o1} - L_{o3}}{2(L_{o1} + L_{o3})}. \quad (3)$$

It is clear that if the total CM voltage V_{tCM} keeps constant, no CM current flows through the converter. For a well-designed circuit with symmetrically structured magnetics, normally L_{o1} is equal to L_{o3}. During the active stage of the positive half-line cycle, V_{1N} is equal to V_{dc}, while V_{3N} is equal to 0. Hence, the total CM voltage can be calculated as

$$V_{tCM} = \frac{V_{1N} + V_{3N}}{2} + (V_{1N} - V_{3N}) \cdot \frac{L_{o1} - L_{o3}}{2(L_{o1} + L_{o3})} = \frac{V_{dc}}{2}. \quad (4)$$

During the freewheeling stage of the positive half-line cycle, under the condition that S1 and S3 share the dc-link voltage equally when they are simultaneously turned OFF, one can obtain

$$V_{1N} = V_{3N} = \frac{V_{dc}}{2} \quad (5)$$

Therefore, the total CMvoltage during the freewheeling stage is calculated as

$$V_{tCM} = \frac{V_{1N} + V_{3N}}{2} + (V_{1N} - V_{3N}) \cdot \frac{L_{o1} - L_{o3}}{2(L_{o1} + L_{o3})} = \frac{V_{dc}}{2} \quad (6)$$

Equations (4) and (6) indicate that the total CM voltage keeps constant in the whole positive half-line cycle. As a result, no CM current is excited. Similarly, during the whole negative half-line cycle, the CM leakage current mode is exactly the same as the one during the positive half-line cycle; the only difference is the activation of different devices. The total CM voltage in the negative half-line cycle is also equal to $V_{dc}/2$. Therefore, in the whole grid cycle the total CM voltage keeps constant, minimizing CM ground leakage current.

PHOTOVOLTAIC (PV) SYSTEM
In the crystalline silicon PV module, the complex physics of the PV cell can be represented by the equivalent electrical circuit shown in Fig. 5. For that

equivalent circuit, a set of equations have been derived, based on standard theory, which allows the operation of a single solar cell to be simulated using data from manufacturers or field experiments.
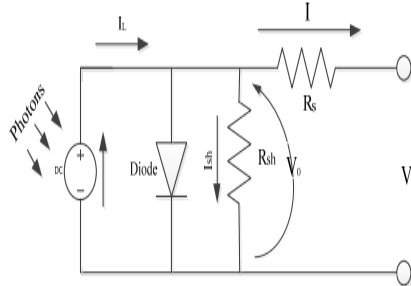

Fig.8 Equivalent electrical circuit of a PV module

The series resistance RS represents the internal losses due to the current flow. Shunt resistance Rsh, in parallel with diode, this corresponds to the leakage current to the ground. The single exponential equation which models a PV cell is extracted from the physics of the PN junction and is widely agreed as echoing the behavior of the PV cell

$$I = I_L - I_K \left(exp \frac{(V + R_s I)}{V_t} - 1 \right) - \frac{(V + R_s I)}{R_{sh}}$$ (7)

The number of PV modules connected in parallel and series in PV array are used in expression. The Vt is also defined in terms of the ideality factor of PN junction (n), Boltzmann's constant (KB), temperature of photovoltaic array (T), and the electron charge (q). applied a dynamical electrical array reconfiguration (EAR) strategy on the photovoltaic (PV) generator of a grid-connected PV system based on a plant-oriented configuration, in order to improve its energy production when the operating conditions of the solar panels are different. The EAR strategy is carried out by inserting a controllable switching matrix between the PV generator and the central inverter, which allows the electrical reconnection of the available PV modules.

SIMULATION RESULTS

Here the simulation is carried out by three different cases 1) proposed inverter 2) under fault condition

(line to ground) 3) proposed inverter under Fault compensation
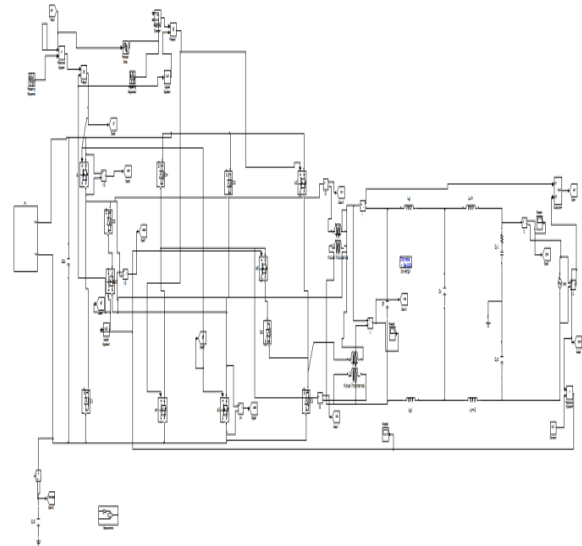
1) Proposed inverter

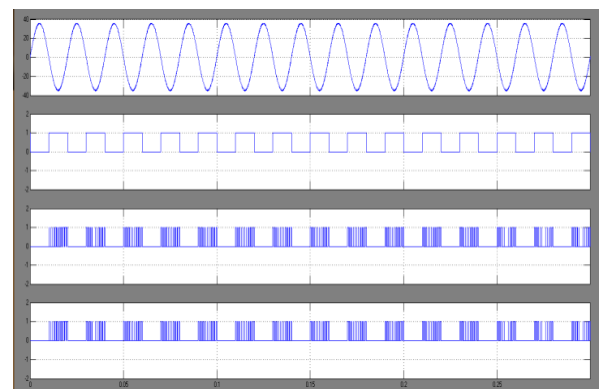Fig.9 Matlab/simulink model of proposed inverter

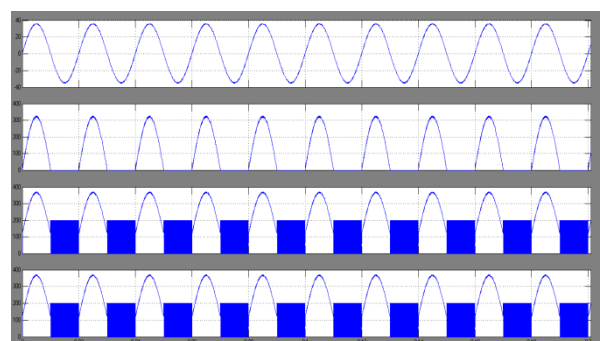Fig.10 Switch gating signals in grid cycle

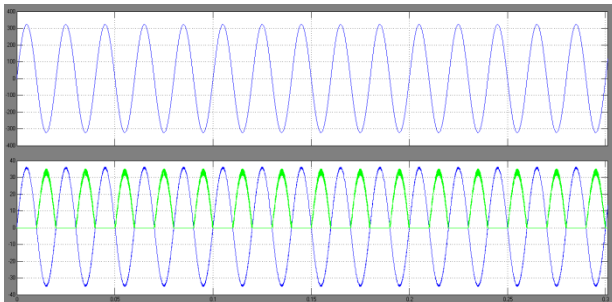Fig.11 Drain–source voltage waveforms of the switches S1, S3, and S5 in grid cycle

Fig.12 simulated waveforms of ground potential V_{EN}, grid current, and current of inductor Lo 1
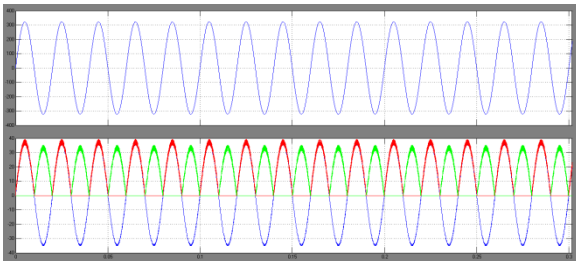

Fig.13 simulated waveforms of grid current and the inductor currents i_{L01} and i_{Lo2}
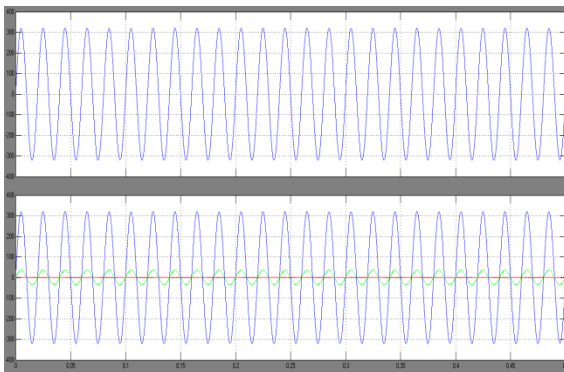

Fig.14 Leakage current test waveforms

CONCLUSION

In this concept Fault Analysis of a Photovoltaic based Single Phase Grid Connected Transformerless Inverter is performance is tested under with fault and fault compensation. A high reliability and efficiency inverter for transformerless PV grid-connected power generation systems is presented in this paper. Ultra high efficiency can be achieved over a wide output power range by reliably employing superjunction MOSFETs for all switches since their body diodes are never activated and no shoot-through issue leads to greatly enhanced reliability. Low ac output current distortion is achieved because dead time is not needed at PWM switching commutation instants and grid-cycle zero-crossing instants. The higher operating frequencies with high efficiency enables reduced cooling requirements and results in system cost savings by shrinking passive components. The proposed converter tested under fault conditions and that fault compensated with FCL.

REFERENCES

[1] J. S. Lai, "Power conditioning circuit topologies," IEEE Ind. Electron. Mag., vol. 3, no. 2, pp. 24–34, Jun. 2009.

[2] S. B. Kjaer, J. K. Pedersen, and F. Blaabjerg, "A review of single-phase grid-connected inverters for photovoltaic modules," IEEE Trans. Ind. Appl., vol. 41, no. 5, pp. 1292–1306, Sep./Oct. 2005.

[3] M. Calais, J.Myrzik, T. Spooner, and V. G. Agelidis, "Inverters for singlephase grid connected photovoltaic systems—An overview," in Proc. IEEE Annu. Power Electron. Spec. Conf., 2002, vol. 2, pp. 1995–2000.

[4] Y. Xue, L. Chang, S. B. Kjaer, J. Bordonau, and T. Shimizu, "Topologies of single-phase inverter for small distributed power generators: An overview," IEEE Trans. Power Electron., vol. 19, no. 5, pp. 1305–1314, Sep. 2004.

[5] Q. Li and P.Wolfs, "A review of the single phase photovoltaic module integrated converter topologies with three different DC link configurations," IEEE Trans. Ind. Electron., vol. 23, no. 23, pp. 1320–1333, Apr. 2008.

[6] J. M. A. Myrzik and M. Calais, "String and module integrated inverters for single-phase grid connected photovoltaic systems-A review," in Proc. IEEE Bologna Power Tech Conf., Bologna, Italy, Jun. 2003, pp. 430–437.

[7] F. Schimpf and L. E. Norum, "Grid connected converters for photovoltaic, state of the art, ideas for improvement of transformerless inverters," presented at the Nordic Workshop Power Ind. Electron., Espoo, Finland, Jun. 2008.

[8] R. Gonzalez, J. Lopez, P. Sanchis, and L. Marroyo, "Transformerless inverter for single-phase photovoltaic systems," IEEE Trans. Power Electron., vol. 22, no. 2, pp. 693–697, Mar. 2007.

[9] H. Schmidt, C. Siedle, and J. Ketterer, "DC/AC converter to convert direct electric voltage into alternating voltage or into alternating current," U.S. Patent 7046534 B2, May 2006.

[10] M. Victor, F. Greizer, S. Bremicker, and U. Hubler, "Method of converting a direct current voltage of a source of direct current voltage, more specifically of a photovoltaic source of direct current voltage, into an alternating current voltage," U.S. Patent 7411802 B2, Aug. 2008.

[11] SMA Sunny Boy 8000TL-US datasheet. [Online]. Available: http://www.sma-america-.com

[12] W. Yu, J. S. Lai, H. Qian, and C. Hutchens, "High-efficiency MOSFET inverter with H6-type configuration for photovoltaic non-isolated AC-module applications," IEEE Trans. Power Electron., vol. 56, no. 4, pp. 1253–1260, Apr. 2